Supporting Information

Visualizing the fluorescence of AgPt NCs by an asymmetrical pseudo-ligand exchange method

Lizhong He [a, b *], Tingting Dong [c], Xiaoyang Hu [d] and Zibao Gan [d *]

a: School of Materials Science & Engineering, Xi'an Polytechnic University, Xi'an 710048, PR China;

b: Institute of Solid State Physics, Chinese Academy of Sciences, Hefei 230031, PR China;
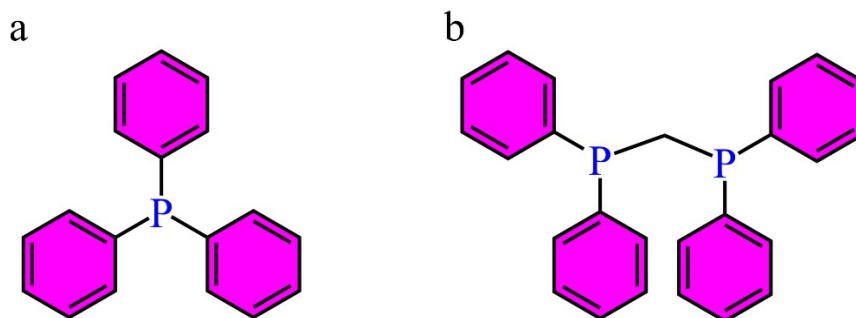
Email: lzhe@xpu.edu.cn

c: School of Environmental Science and Engineering, Shaanxi University of Science and Technology, Xi'an 710021, PR China.
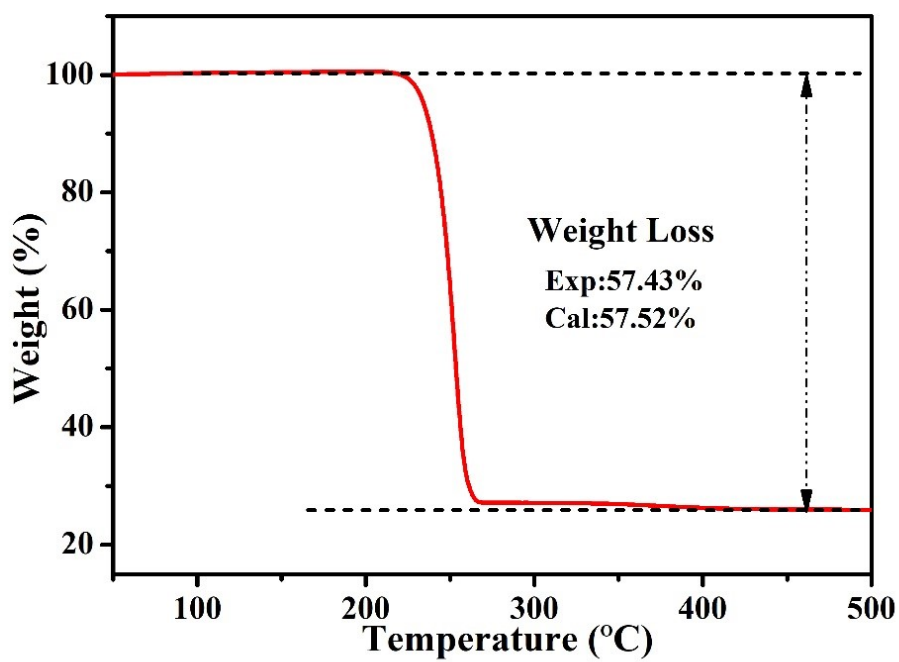
d: School of Chemistry and Chemical Engineering, Linyi University, West Side of North Section of Industrial Avenue, Linyi, 276000, PR China；

Email: ganzibao@lyu.edu.cn

1. Supporting Figures

a

b

Figure S1. The structures of (a) PPh$_3$ and (b) dppm, respectively.

Figure S2. TGA of Ag$_{16}$Pt NC.
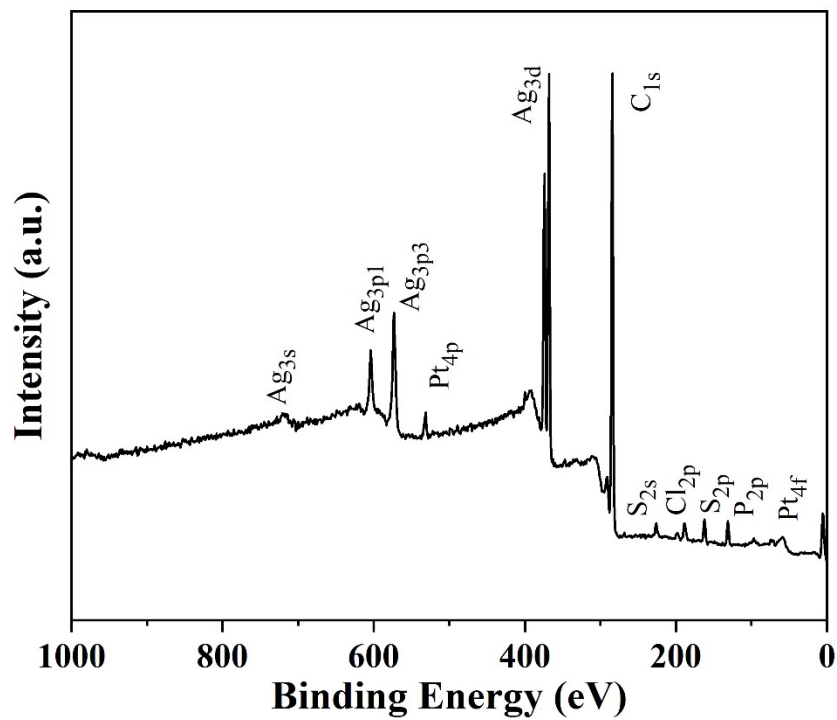
Figure S3. XPS spectrum of $Ag_{16}Pt$ NC.
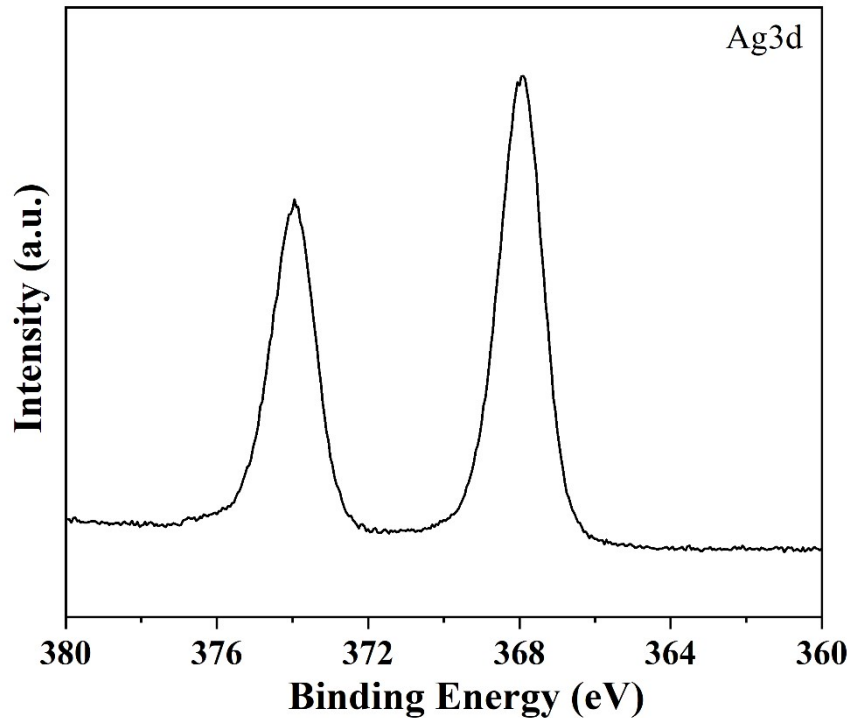
Figure S4. XPS spectrum of Ag_{3d} in the $Ag_{16}Pt$ NC.
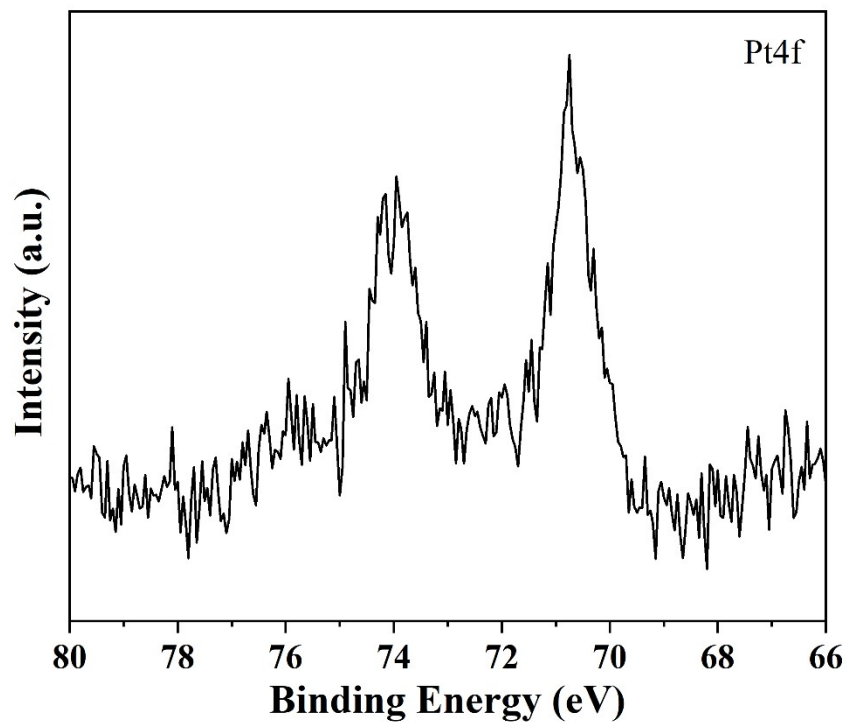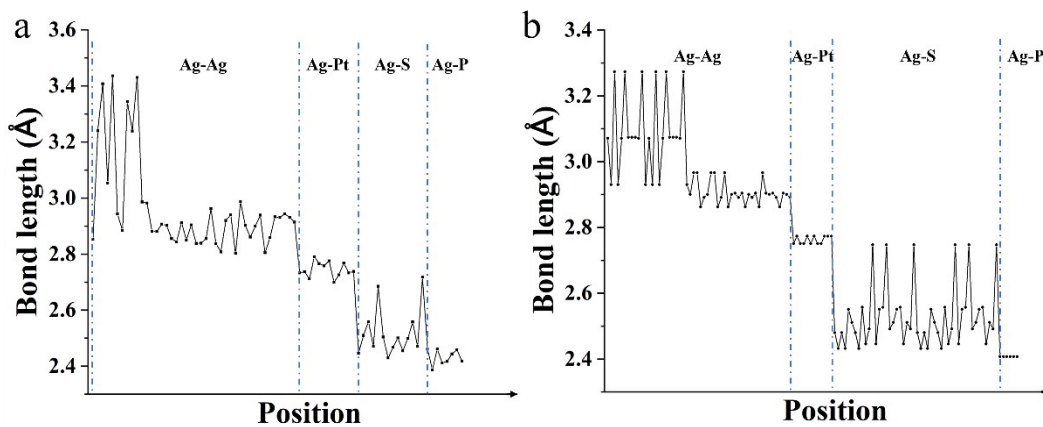
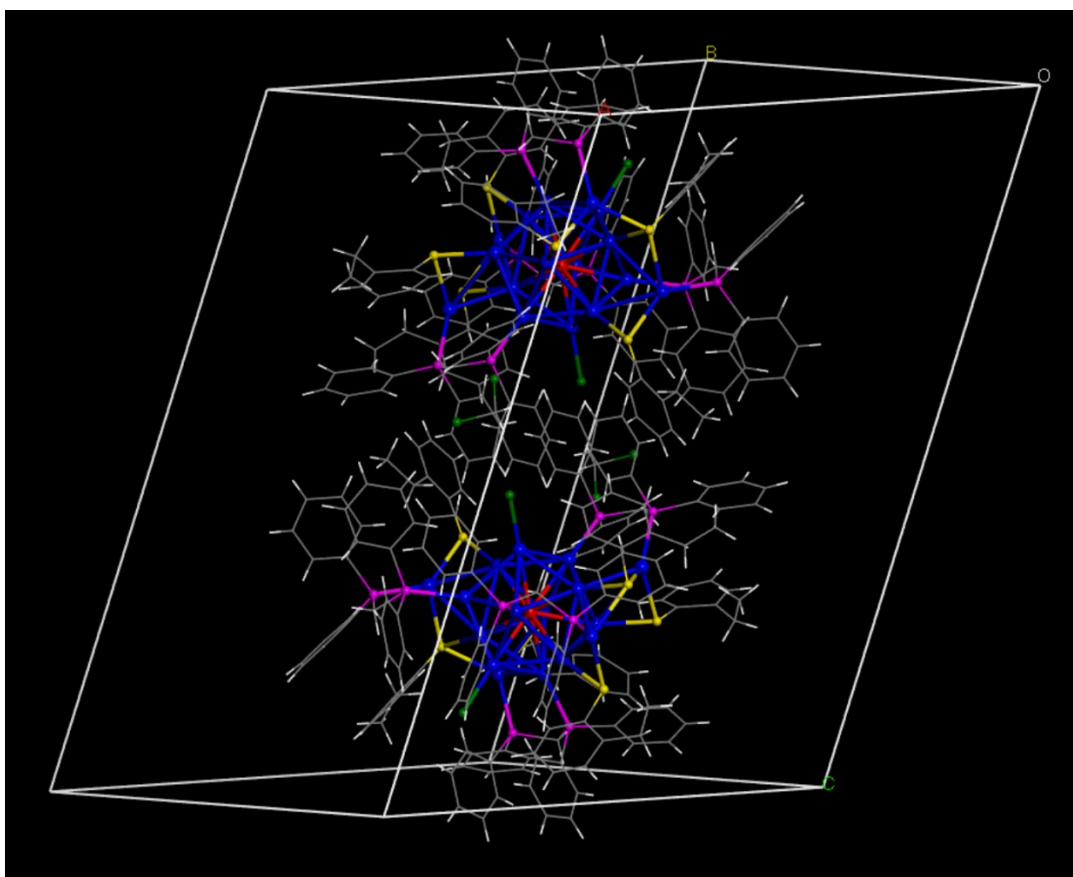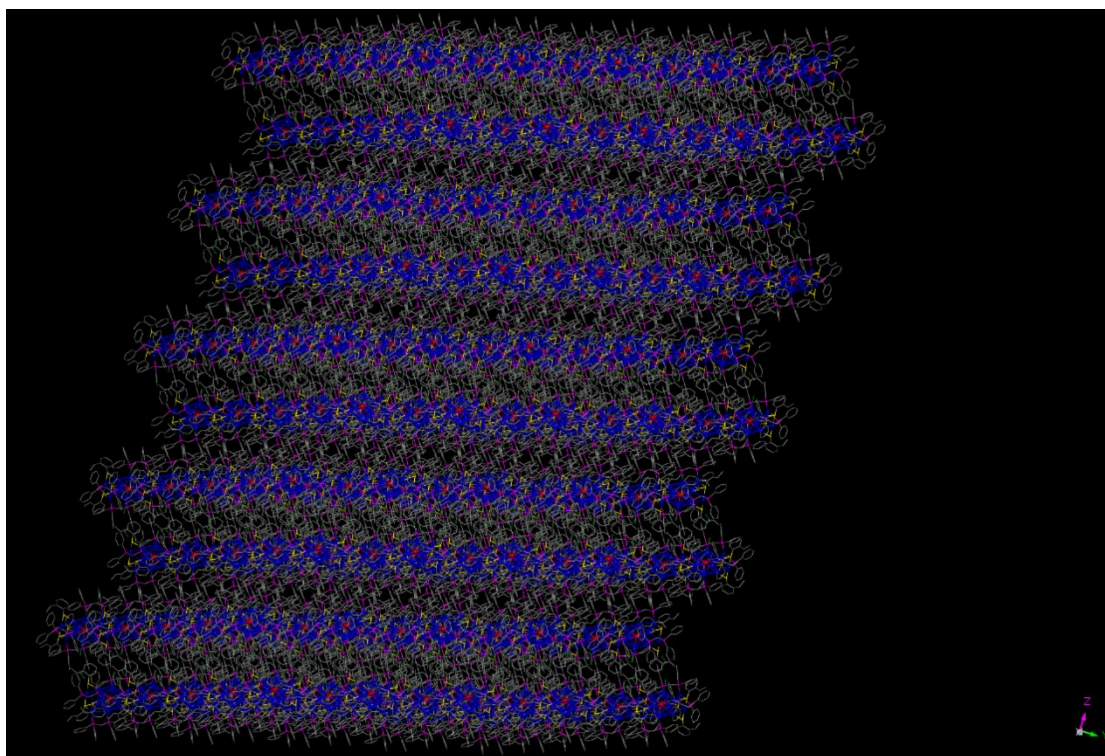**Figure S5.** XPS spectrum of Pt_{4f} in the $Ag_{16}Pt$ NC.

Figure S6. Bond lengths of (a) $Ag_{16}Pt$ and (b) $Ag_{26}Pt$ NCs, respectively.

Figure S7. Unit cell of the three-dimensional structure of the $Ag_{16}Pt$ NCs in a ball and stick model. Color codes: blue Ag, red Pt, yellow S, magenta P, gray C and White H.

Figure S8. Multilayer stacking structure of the Ag$_{16}$Pt NCs (viewed from X direction).

Color code: blue Ag; red, Pt; yellow, S; magenta, P; gray, C; white, H.
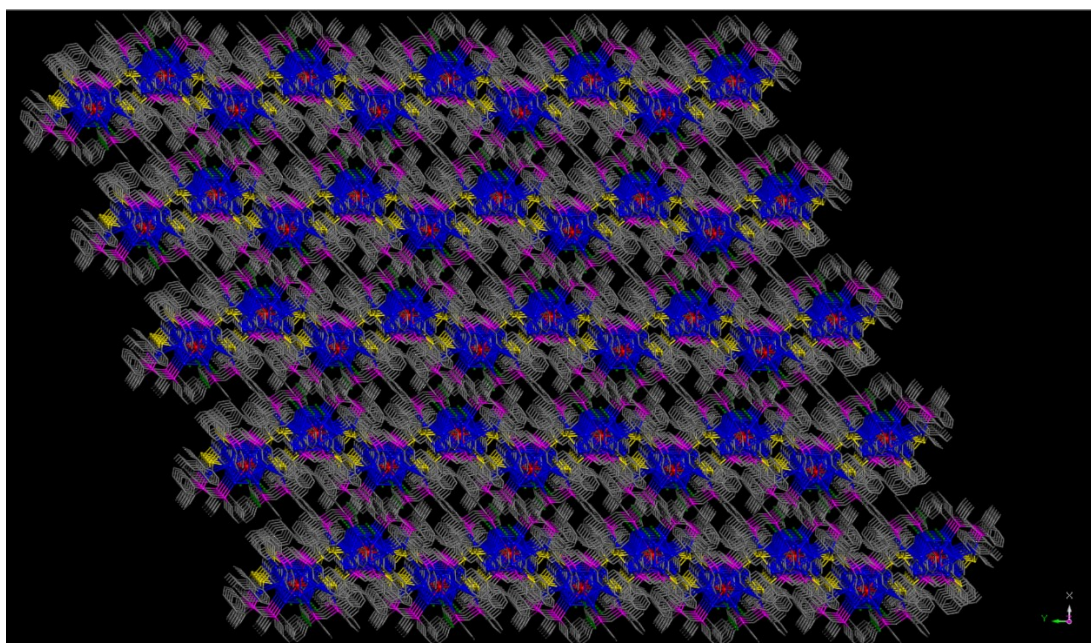
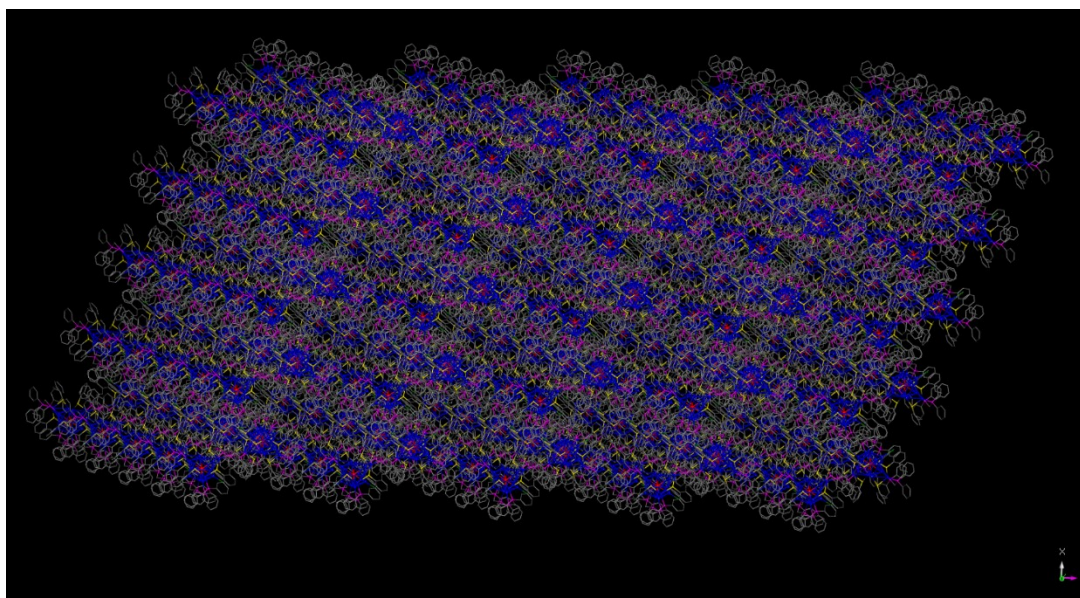**Figure S9.** Multilayer stacking structure of the Ag$_{16}$Pt NCs (viewed from Z direction).

Color code: blue Ag; red, Pt; yellow, S; magenta, P; gray, C; white, H.
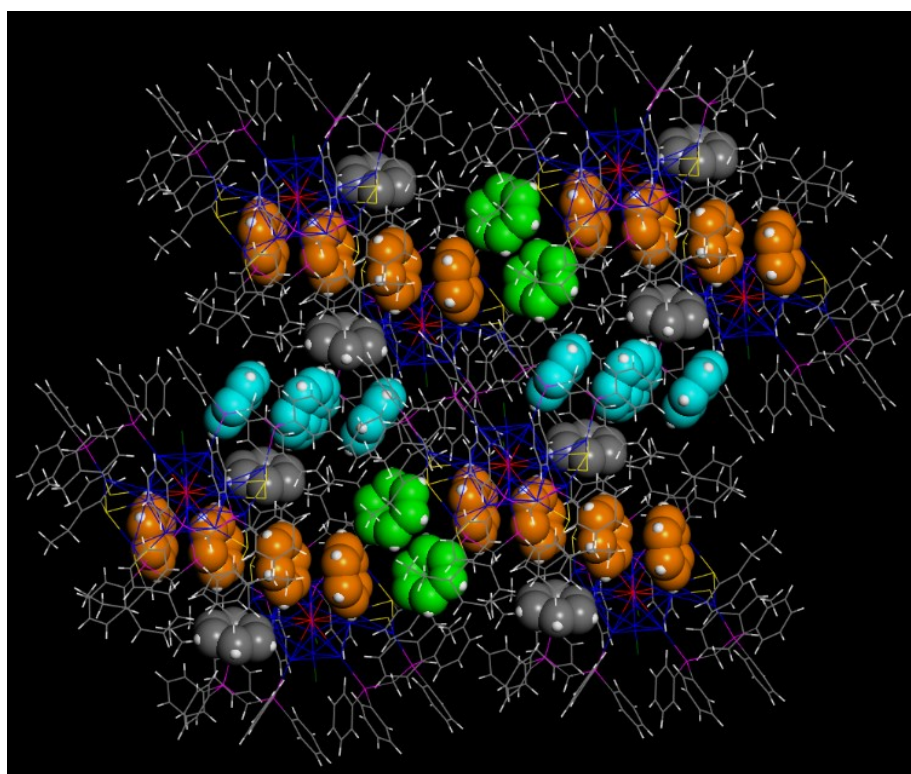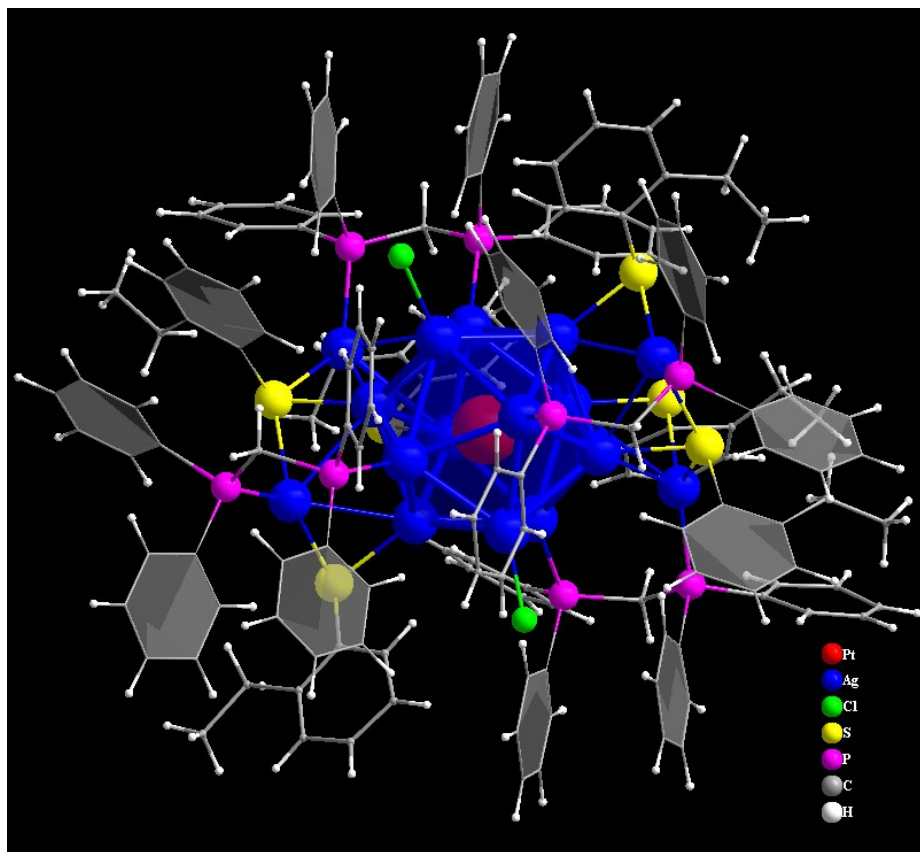
Figure S10. Multilayer stacking structure of the $Ag_{16}Pt$ NCs (viewed from Y direction). Color code: blue Ag; red, Pt; yellow, S; magenta, P; gray, C; white, H.

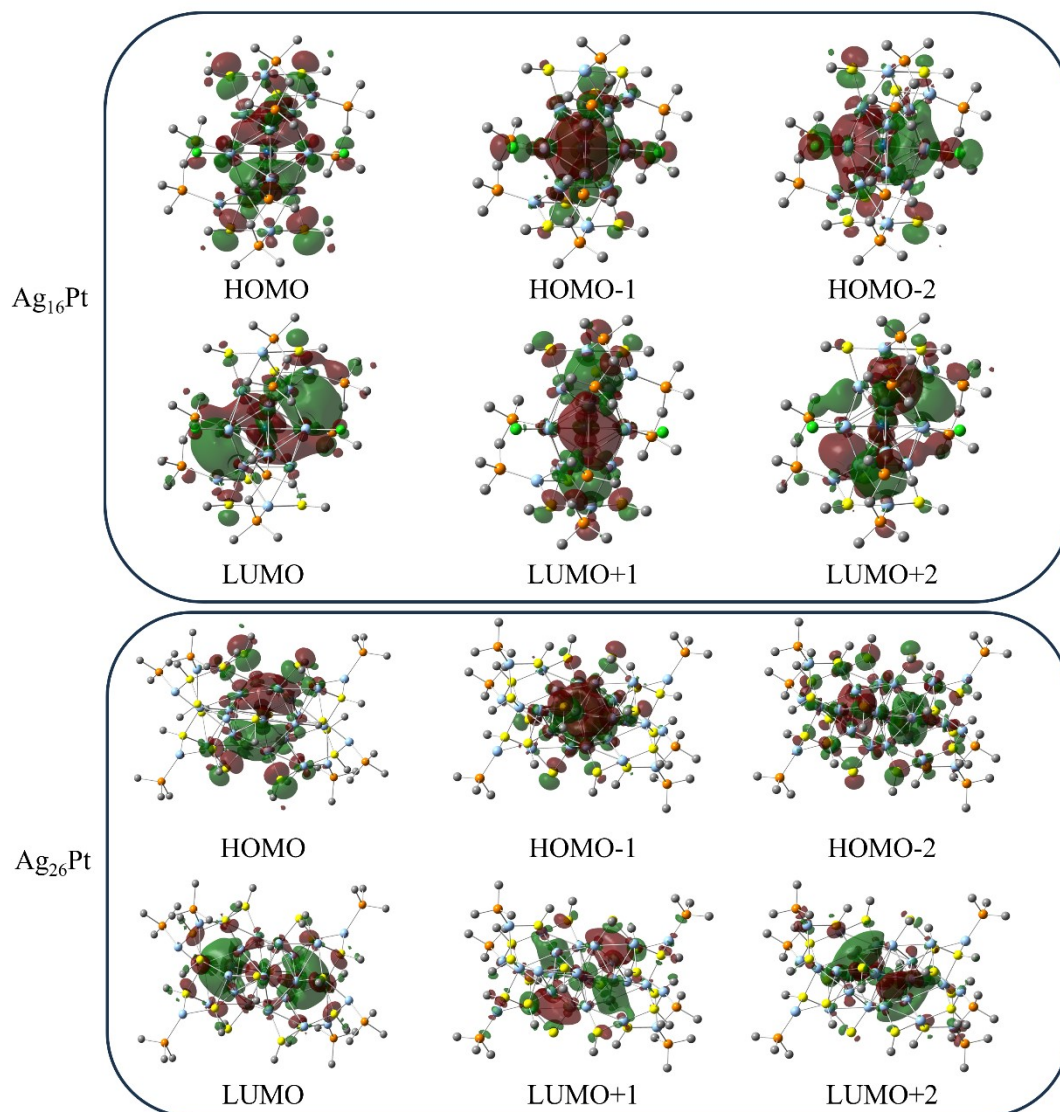**Figure S11.** The inter-nanocluster C-H···π, and π···π interactions in the $Ag_{16}Pt$ NCs. Color codes: red, Pt; blue, Ag; yellow, S; gray, green, brown and light blue, C; white, H.
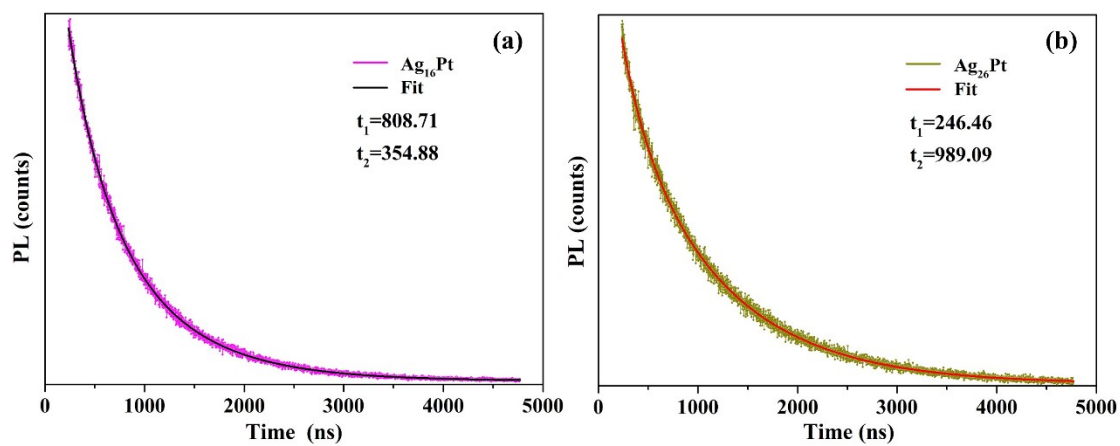
Figure S12. The intra-nanocluster π···π interactions in the Ag$_{16}$Pt NC.

Figure S13. Electron densities of the HOMO, HOMO-1, HOMO-2 and LUMO, LUMO+1, LUMO+2 of the $Ag_{16}Pt$ and the $Ag_{26}Pt$ NCs.

Figure S14. Fluorescence decay profiles of the Ag$_{16}$Pt and the Ag$_{26}$Pt NCs.
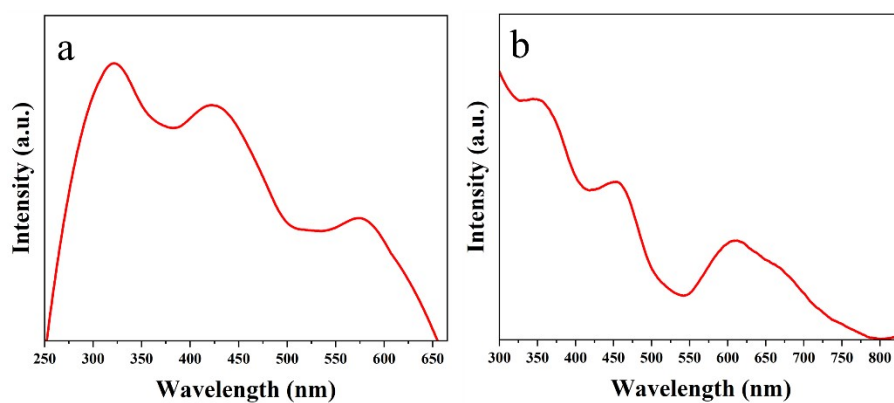
Figure S15. The excitation spectra of Ag$_{16}$Pt and Ag$_{26}$Pt NCs, respectively.
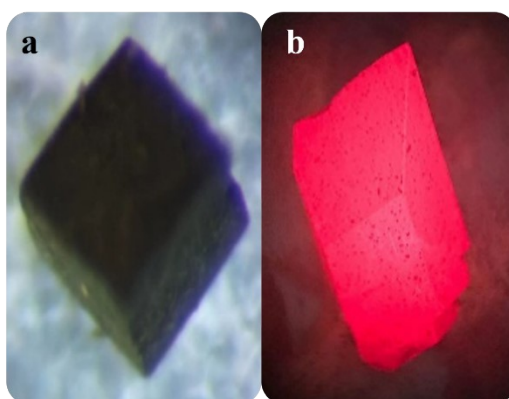
Figure S16. The optical photographs of (a) Ag$_{26}$Pt and (b) Ag$_{16}$Pt NC crystals under 365 nm UV light irradiation.

2. Single crystal data

2.1 Single crystal data of Ag$_{16}$Pt NC

Empirical formula	C$_{148}$ H$_{142}$ Ag$_{16}$ Pt$_1$ S$_6$ P$_8$ Cl$_2$
Formula weight	4522.46
Temperature/ K	150
Wavelength	1.34139 Å
Crystal system	triclinic
Space group	P-1
Unit cell dimensions	a = 18.450(6) Å α=75.225(11)
	b= 18.992(6) Å β=73.008(10)
	c = 29.482(9) Å γ=64.526(11)
Volume/ Å^3	8819(5)
Z	2
ρ_{calc}g/cm^3	1.703
μ/mm^{-1}	12.134
F(000)	4388.0
Index ranges	-22<=h<=22, -23<=k<=23, -35<=l<=36
Reflections collected	127207
Independent reflections	33557 [R$_{int}$ = 0.0909, R$_{sigma}$=0.0831]
2Θrange for data collection	4.534°- 110.668°
Data / restraints / parameters	33557 / 3316 / 1691
Goodness-of-fit on F^2	1.093
Final R indices [I>2sigma(I)]	R$_1$ = 0.0847, wR$_2$ = 0.2419
R indices (all data)	R$_1$ = 0.1073, wR$_2$ = 0.2624
Extinction coefficient	n/a
Largest diff. peak and hole/ e Å^{-3}	3.50 and -3.13